

FAILURE ANALYSIS ON IRRADIATED CLADDINGS SUBJECTED TO LONG-TERM DRY INTERIM STORAGE

Uwe Zencker¹, Mohan Reddy Gaddampally², Holger Völzke³

¹ Dr.-Ing., Bundesanstalt für Materialforschung und -prüfung, Berlin, Germany (uwe.zencker@bam.de)

² formerly Bundesanstalt für Materialforschung und -prüfung (BAM), Berlin, Germany

³ Dr.-Ing., Bundesanstalt für Materialforschung und -prüfung (BAM), Berlin, Germany

ABSTRACT

Long-term dry interim storage may adversely affect the mechanical properties of spent fuel rods, possibly resulting in a reduced resilience during handling or transport after storage. The cladding is the first barrier for the spent fuel pellets. An established method for characterising the cladding material is the ring compression test (RCT), in which a small, cylindrical sample of the cladding tube is subjected to a compressive load. Radial hydrides may precipitate in zirconium-based alloys (Zircaloy) under pre-storage drying and during slow cooling, which result in embrittlement of the cladding material and eventually a possible sudden failure of cladding integrity under additional mechanical loads. The focus of the presented research is on the development of appropriate numerical methods for predicting the mechanical behaviour and identification of limiting conditions to prevent brittle fracture of Zircaloy claddings. A modelling approach based on cohesive zones is explained which is able to reproduce the propagation of cracks initiated at radial hydrides in the zirconium matrix. The developed methods are applied to defueled samples of cladding alloy ZIRLO[®], which were subjected to a thermo-mechanical treatment to reorient existing circumferential hydrides to radial hydrides. A selected sample showing sudden load drops during a quasi-static ring compression test is analysed by means of fracture mechanics for illustrative purposes. Based on the developed fracture mechanics approach, not only the deformation behaviour but also the failure behaviour of irradiated as well as unirradiated Zircaloy claddings with radial hydrides under RCT loading conditions can be adequately described.

INTRODUCTION

The mechanical properties of spent fuel claddings made of zirconium-based alloys can be impaired by long-term dry interim storage. Cladding failure, possibly even brittle fracture, can occur if mechanical stress is applied during handling or transport of the fuel assemblies. High temperatures during vacuum drying and at the beginning of interim storage of the cask can cause existing zirconium hydrides to dissolve. During subsequent slow cooling under pressure-induced tensile hoop stresses in the cladding, radial hydrides can precipitate that may result in embrittlement of the cladding material; see Billone et al. (2013a). Whether failure occurs under mechanical load depends heavily on the actual stress state and the morphology of the hydrides. In particular, long continuous radial hydride structures can lead to severe embrittlement of the cladding. If this happens, failure is possible even with only minor deformation of the fuel rod.

A potentially hazardous load case for cladding tubes with radial hydrides is a fuel rod pinch-type loading. This scenario can be represented under laboratory conditions by the ring compression test (RCT) on a small cylindrical sample. Billone et al. (2012) conducted RCT baseline studies of high-burnup (HBU) fuel cladding alloy ZIRLO[®] to investigate its deformation behaviour. Later, Billone et al. (2013b) performed quasi-static RCTs on ZIRLO[®] samples with radial hydrides to characterise brittle failure.

Since the stress state in the sample is not homogeneous during the RCT, finite element analyses (FEA) can help to understand the failure behaviour. Stress-plastic strain curves can be obtained from baseline studies (without radial hydrides) to simulate the sample deformation. Martin et al. (2013) and Gómez et al. (2017a) demonstrated the use of a cohesive zone in a finite element model to predict the ductile failure of pre-hydrated unirradiated RCT samples. Simbruner et al. (2022) improved the method and applied

it to irradiated M5[®] cladding samples with radial hydrides to simulate brittle fracture under RCT conditions by cohesive zone modelling.

In this paper, the cohesive zone modelling is applied to a different material, namely the irradiated cladding alloy ZIRLO[®], to demonstrate the general material-independent applicability of the method to simulate brittle fracture of RCT samples from defueled fuel rods. The cladding tube was subjected to a thermo-mechanical treatment to reorient existing circumferential hydrides to radial hydrides. A sample showing abrupt load drops during a ring compression test was exemplarily selected. The failure behaviour is characterised by fracture mechanics parameters.

RING COMPRESSION TEST

The investigated material is the cold-worked, stress-relieved annealed zirconium alloy ZIRLO[®]. The samples were cut from segments of about 80 mm in length, which were taken from a defueled fuel rod with burnup of 68 GWd/MTU. Segment 105A was used for baseline tests to investigate the microstructure of the material and to determine stress-strain properties as documented by Billone et al. (2012). The average outer diameter of the corroded cladding was 9.53 ± 0.02 mm, and the outer diameter of the cladding metal was 9.44 ± 0.02 mm. The cladding metal wall thickness was 0.54 ± 0.01 mm. The corroded cladding had an average hydrogen content of 530 wppm (weight parts per million). Metallographic studies of samples from this segment have shown that there were a few radial hydrides among predominantly circumferential hydrides.

Segment 105C was taken from the same HBU fuel rod from which the as-irradiated segment (105A) was sectioned. Both ends of the segment were closed with weld seams to create a rodlet. This rodlet was subjected to a radial hydride treatment (RHT) to simulate drying and storage of the fuel rod. The sealed and pressurized rodlet was heated to 400 °C to dissolve existing hydrides. The temperature was held for one hour. The rodlet was then cooled slowly at 5°C/hour to 200°C, where essentially all the hydrogen re-precipitated as hydrides, and afterwards at a faster rate to room temperature (RT). Metallographic studies have shown that this treatment creates a network of circumferential and radial hydrides, but with pronounced radial hydride structures.

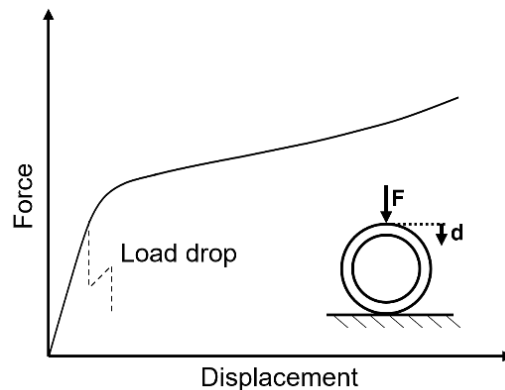


Figure 1. Schematic force-displacement behaviour in RCT.

In the ring compression test, a small cylindrical sample of the cladding is subjected to a compressive load. Figure 1 depicts the experimental setup and the expected force-displacement curve. The continuous line represents the test result of a ring sample without radial hydrides. The dashed line illustrates a load drop due to brittle failure of the sample, which can occur in several steps. This type of failure is usually seen in the presence of pronounced, long radial hydrides. All tests considered here were carried out at room temperature (23 °C) in displacement-controlled mode at constant loading rate of 5 mm/s to the maximum displacement of 1.7 mm using an Instron 8511 servo-hydraulic material testing machine.

FINITE ELEMENT ANALYSIS

Based on the experimental data, a finite element analysis (FEA) was carried out to understand the complex interaction between the stress state, hydride structure, and initiation of cracks. The sudden load drops observed in the force-displacement diagram are the result of fast propagating cracks in the hydride structure, which should be reproduced by the FEA model. The model was simplified by assuming plane strain conditions. The commercial code ABAQUS[®] in quasi-static analysis mode was used for all calculations. The sample rests on a lower support plate that is assumed to be rigid. The deformation is caused by a movable upper loading plate, also assumed to be rigid, which is pressed onto the top of the sample. The solid section of the ring consists of plane strain elements with eight nodes, quadratic interpolation, and reduced integration (ABAQUS[®] element type CPE8R). At the 12 o'clock position of the ring, a 1 μm wide gap was modelled along the wall thickness. This gap was filled with a cohesive section of the same thickness. Tie constraints were used to connect the cohesive section and the surrounding mesh. The cohesive section was meshed using two-dimensional four-node cohesive elements (ABAQUS[®] element type COH2D4). It is important to set the length of the individual sample as the out-of-plane width of the finite elements, as this scales the calculation result.

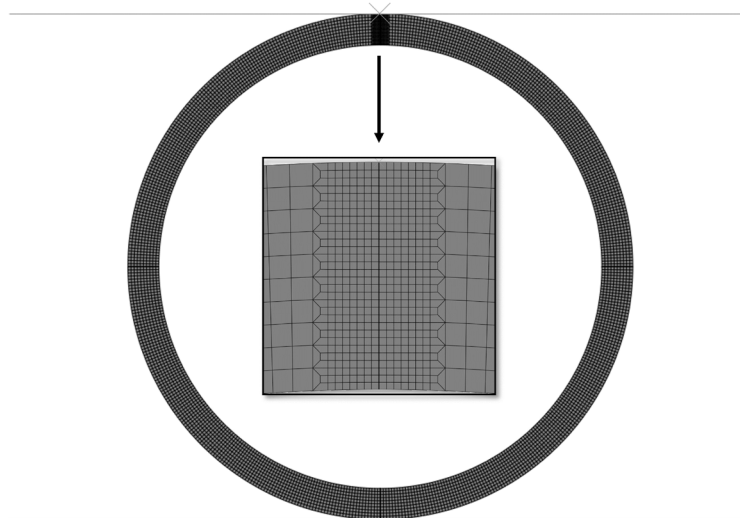


Figure 2. Finite element mesh employed for cohesive zone modelling.

The prescribed displacement of the upper plate applied the load, which was determined as the reaction force. All degrees of freedom of the lower plate were constrained. ABAQUS[®] surface-to-surface contact was used to model the contact between solid or rigid parts. The finite element model considered non-linear geometry because large deformations were expected. An elastic-plastic model with von Mises plasticity described the material behaviour. Coulomb friction with a friction coefficient of 0.125 based on Arsene and Bai (1996) was used for all numerical contacts. Figure 2 shows the complete finite element mesh with a detail around the cohesive zone (CZ). In most of the ring, 10 finite elements were used across the wall thickness. The mesh was refined around the 12 o'clock position to better reflect the complex stress state in the sample. The cohesive zone itself was very finely discretised with 1000 cohesive elements in order to split the crack propagation into small steps and thus obtain a smooth and stable calculation result.

The investigation described involves a two-stage FEA approach. In the first stage, a baseline RCT was analysed numerically using the sample 105A9 (from segment 105A before RHT) to get the relevant stress-plastic strain relation (flow curve) by an automated inverse analysis method. In the second stage, a RCT with pronounced radial hydride structures was simulated using sample 105C4 (from segment 105C after RHT) to examine the failure along radial hydrides. In this calculation, the deformation behaviour of the sample was based on the flow curve determined in the first stage.

Evaluation of Mechanical Properties

An appropriate stress-plastic strain curve is required so that the simulated deformation behaviour of the sample matches the observed experimental behaviour as closely as possible. For that purpose, an iteration algorithm was developed based on Gómez et al. (2017b). The initial force-displacement curve is calculated numerically with a stress-plastic strain curve $(\sigma_i, \varepsilon_i^p)$ with von Mises Stress σ_i and equivalent plastic strain ε_i^p assumed for an ideal plastic case ($i = 0$). The stress σ_i is then modified according to

$$\sigma_{i+1}(\varepsilon^p) = \sigma_i(\varepsilon^p) \frac{F_{exp}(d)}{F_i(d)} \quad (1)$$

With the measured (experimental) force F_{exp} , the calculated force F_i and displacement d , where index $i = 0, 1, \dots$ denotes the iteration step to minimise the deviations between the numerical and experimental results. The difficulty with this approach is the implicit dependency of equivalent plastic strain and displacement. In order to establish a relationship between these two variables, the parameterised representation

$$d = d_{min} + (d_{max} - d_{min}) t \quad (2)$$

is introduced, where the auxiliary parameter t varies from 0 to 1. The displacement at which the linearity of the force-displacement curve ends is referred to as d_{min} and depends on the individual test. The maximum displacement in the simulation is denoted by d_{max} . The relationship

$$\varepsilon^p = \varepsilon_{max}^p t^\alpha \quad (3)$$

is used to interpolate the equivalent plastic strain, whereby the value of the exponent α is typically between 0.5 and 3. Because each integration point of each finite element in the model has a different local equivalent plastic strain, the maximum value over all integration points is meant here. The equivalent plastic strain ε_{max}^p at maximum force can be determined in the RCT calculation carried out for iteration step i . The exponent is derived using the course of the equivalent plastic strain $\varepsilon^p(t)$ from the simulation. In each iteration step i , a new exponent is adjusted using the least squares method. By inserting Eqs. (2) and (3) into the iteration rule Eq. (1), an explicit relation can be established depending on the parameter t . Thus, with the new stress-plastic strain curve $(\sigma_{i+1}, \varepsilon_{i+1}^p)$, an iteration process can be carried out until the numerical force-displacement curve matches the experimental curve, cf. Figure 3.

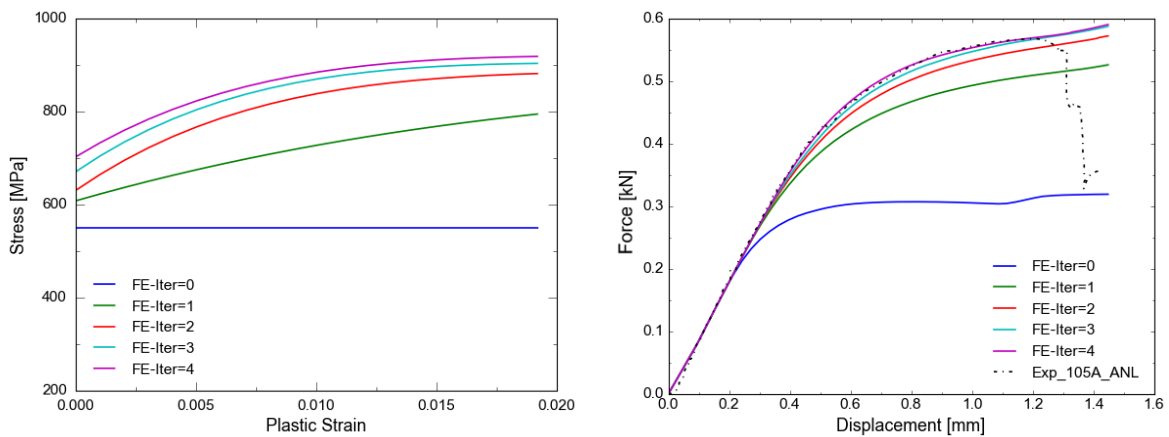


Figure 3. Iterative procedure to fit the experimental force-displacement curve.

The iterative algorithm was implemented as Python code using the ABAQUS[®]-Python interface for automatic data transfer. The linear elastic behaviour was modelled with a Young's modulus E of 88 GPa and Poisson's ratio ν of 0.37 from Weck et al. (2015). By comparing the deviation from a linear-elastic calculation and the experiment, the yield stress was determined to be 701.7 MPa. Due to the symmetry, only half of the ring was modelled for the calculations to adjust the flow curve in order to reduce the computing time.

Cohesive Zone Modelling

A cohesive zone model (CZM) with a traction-separation law was adapted to describe the failure process along radial hydride structures in irradiated cladding samples. The traction-separation approach consists of three parts: linear-elastic behaviour, damage initiation, and damage evolution. Figure 4 shows a simple traction-separation curve with triangular shape. An elastic stiffness coefficient k describes the material response in the elastic part where the separation δ is smaller than a given value δ_1 . Young's modulus of the surrounding bulk material is divided by the initial thickness of the cohesive interface, which yields $k = 88000$ GPa/mm for the elastic stiffness of the cohesive interface. Once an applied tensile stress σ_c reaches the cohesive strength σ_{c0} , damage is initiated within the cohesive element. As the separation δ of the element increases beyond δ_1 , the stiffness decreases monotonically, which is controlled by the scalar damage variable D :

$$\sigma_c = k \delta (1 - D) \quad \text{with} \quad 0 \leq D \leq 1 \quad (4)$$

The separation energy dissipated in the damage process is represented by the area under the traction-separation curve as shown in Figure 4 and is denoted as G_C . The degradation behaviour of a cohesive element is therefore determined by the parameters σ_{c0} and G_C for the given triangular traction-separation curve.

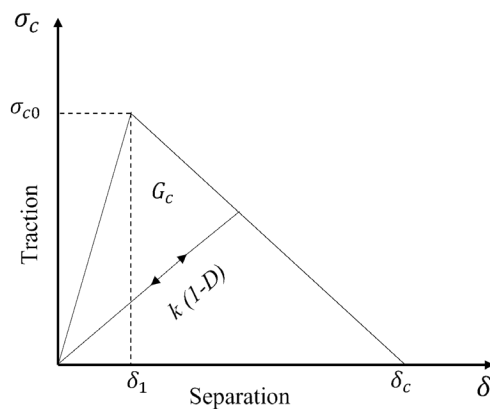


Figure 4. Schematic traction-separation law.

FAILURE ANALYSIS

The failure mechanism of zirconium-based cladding alloys with radial hydrides subjected to RCT loading conditions consists of two different failure modes and was described by Ruiz et al. (2021) based on the analysis of fracture surfaces. Quasi-cleavage along hydride structures was the dominating appearance of the fracture surface and an indicator of brittle failure. Some areas of the fracture surface showed void growth and coalescence associated with ductile failure and crack propagation through the zirconium matrix. Simbruner et al. (2022) mapped the structure of the fracture surface of a RCT sample onto a cohesive zone

to allow modelling of brittle behaviour along the hydrides and ductile behaviour along the zirconium matrix within the same cohesive zone. A separate cohesive law was used for each of the two failure modes. Various matrix-hydride distributions were investigated with assumptions on the size and distance of the hydrides and on the ratio of brittle areas to ductile areas on the fracture surface.

In the present study, the alternating failure due to quasi-brittle fracture at the hydrides and ductile failure of the zirconium matrix segments is considered in a smeared manner, in that the failure mechanisms are not spatially resolved. This results in the approach of an effective cohesive law with only one set of cohesive zone parameters.

The quasi-static RCT on ZIRLO[®] sample 105C4 with radial hydrides, as described by Billone et al. (2013b), was selected for the investigation of the failure behaviour of irradiated ZIRLO[®] cladding. A crack was assumed from the inside of the sample along a radial hydride structure at the 12 o'clock position, where a cohesive zone was inserted into the finite element model. The stress-plastic strain curve based on the RCT with sample 105A9 at room temperature was given as input to describe the overall deformation behaviour.

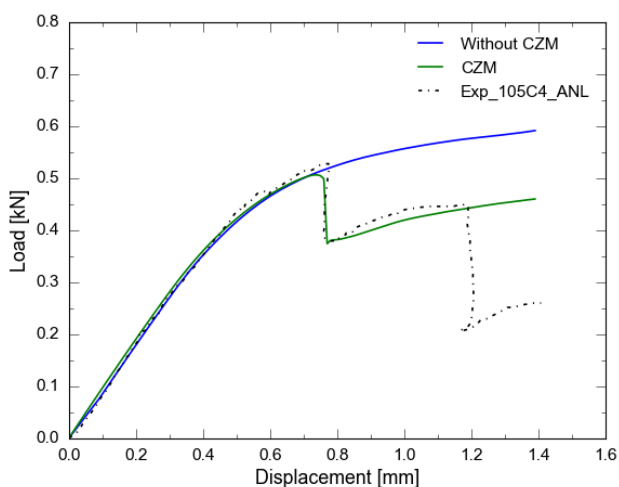


Figure 5. FEA results with and without CZM compared to the test result.

Figure 5 shows the test result together with calculation results with and without a cohesive zone. A series of simulations was carried out to determine the cohesive zone parameters for good agreement with the experimental results as given in Table 1. The first major load drop occurred just after the yield point at around 0.75 mm of global displacement. The maximum load calculated in the FEA before crack initiation and the load drop agree well with the experimental results. The simulation result shows a load drop of around 25 %, while the RCT showed a value of around 28 %.

Table 1: Cohesive zone parameters.

Cohesive zone model	σ_{c0} [MPa]	G_C [N/mm]
Effective cohesive law	1010	22.5

The hoop stress in the finite element model at the end of the calculation with opened crack is shown in Figure 6. To consider further load drops, additional cohesive zones are necessary at the 6 o'clock position near the inside and at the 3 and 9 o'clock positions near the outside of the modelled sample. However, the determination if a unique set of cohesive zone parameters may be difficult because of complex interactions between zirconium hydrides and the surrounding zirconium matrix in the fracture zone. Simbruner et al. (2022) have shown that even minor variations in the positioning of ductile patches in the fracture zone can

change the result of the RCT quantitatively and qualitatively. The success of the simulation therefore depends not only on the knowledge of the cohesive parameters, but also on the hydride structure actually present in the sample.

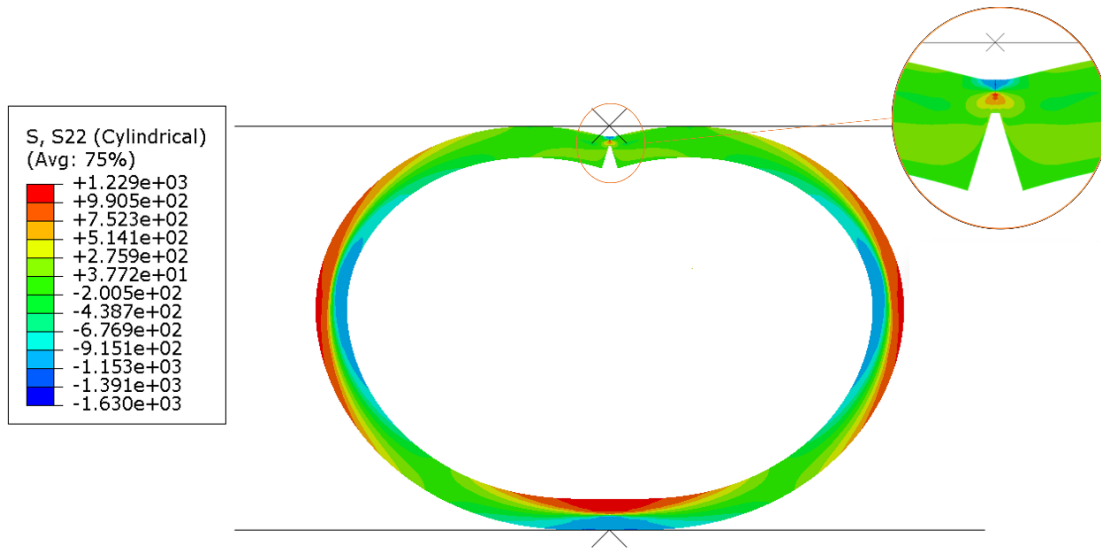


Figure 6. Hoop stress in the finite element model (last increment) and the crack opening at 12 o'clock position for a ZIRLO[®] sample with cohesive zone modelling.

CONCLUSION

Irradiated ZIRLO[®] samples were numerically analysed in the RCT at room temperature. In the force-displacement diagram, the after-RHT sample showed a distinct load drop at a displacement of around 0.75 mm just above the linear part of the curve, followed by further stepwise load drops. The load drops are associated with the formation of cracks on radial hydrides at locations with the highest tensile hoop stress, either on the inside (12 and 6 o'clock positions) or on the outside (3 and 9 o'clock positions) of the ring-shaped sample. Crack initiation and brittle crack propagation occur at one of these locations if a suitable radial hydride is present at which a fracture-mechanically critical crack tip load occurs in conjunction with the local stress state. This behaviour corresponds to a phenomenon of the weakest link type.

It could be shown that the brittle fracture of cladding samples with radial hydrides can be described with a cohesive zone model if the cohesive parameters are selected appropriately and the hydride morphology is specified. A flow curve of the sample material was generated by an inverse analysis of the ring compression test under the assumption of an isotropic elastic-plastic material. In this way, the deformation behaviour of a sample without radial hydrides could be simulated with sufficient accuracy for the following failure analysis.

The parameters of the cohesive zone model (i.e. the cohesive strength and the separation energy for a given traction-separation law) are proposed as a local two-parameter failure criterion for the safety evaluation of zirconium-based cladding alloys with radial hydrides under RCT loading conditions or fuel rod pinch-type loading respectively. The cohesive parameters can be determined by inverse analysis of the experimental results of samples that fail by fracture in the RCT. The hydride morphology to be used for this depends on the individual hydrogen content and the thermo-mechanical load history of the cladding tube to be analysed. The interpretation of the separation energy as an energy release rate provides a link to classical fracture mechanics.

ACKNOWLEDGEMENT

The authors wish to acknowledge the financial support by the European Union's Horizon 2020 research and innovation programme under grant agreement no. 847593.

REFERENCES

- Arsene, S. and Bai, J. (1996). "A new approach to measuring transverse properties of structural tubing by a ring test," *Journal of Testing and Evaluation*, 24, 386-391.
- Billone, M. C., Burtseva, T. A. and Liu, Y. Y. (2012). *Baseline Studies for Ring Compression Testing of High-Burnup Fuel Cladding*, Report FCRD-USED-2013-000040 (ANL 12/58), Argonne National Lemont, IL.
- Billone, M. C., Burtseva, T. A. and Einziger, R. E. (2013a). "Ductile-to-brittle transition temperature for high-burnup cladding alloys exposed to simulated drying-storage conditions," *Journal of Nuclear Materials*, 433, 431-448.
- Billone, M. C., Burtseva, T. A., Han, Z. and Liu, Y. Y. (2013b). *Embrittlement and DBTT of High-Burnup PWR Fuel Cladding Alloys*, Report FCRD-UFD-2013-000401 (ANL 13/16), Argonne National Laboratory, Lemont, IL.
- Gómez-Sánchez, F. J., Martin-Rengel, M. A., Ruiz-Hervías, J. and Puerta, M. A. (2017a). "Study of the hoop fracture behaviour of nuclear fuel cladding from ring compression tests by means of non-linear optimization techniques," *Journal of Nuclear Materials*, 489, 150-157.
- Gómez-Sánchez, F. J., Martin-Rengel, M. A. and Ruiz-Hervías, J. (2017b). "A new procedure to calculate the constitutive equation of nuclear fuel cladding from ring compression tests," *Progress in Nuclear Energy*, 97, 245-251.
- Martin-Rengel, M. A., Gómez-Sánchez, F. J., Ruiz-Hervías, J. and Caballero, L. (2013). "Determination of the hoop fracture properties of unirradiated hydrogen-charged nuclear fuel cladding from ring compression tests," *Journal of Nuclear Materials*, 436, 123-129.
- Ruiz-Hervías, J., Simbruner, K., Cristobal-Beneyto, M., Perez-Gallego, D. and Zencker, U. (2021). "Failure mechanisms in unirradiated ZIRLO® cladding with radial hydrides," *Journal of Nuclear Materials*, 544, 152668.
- Simbruner, K., Billone, M. C., Zencker, U., Liu, Y. Y. and Völzke, H. (2022). "Brittle failure analysis of high-burnup PWR fuel cladding alloys," *Trans., 26th International Conference on Structural Mechanics in Reactor Technology (SMiRT)*, Berlin, Germany.
- Weck, P. F., Kim, E., Tikare, V. and Mitchell, J. A. (2015). "Mechanical properties of zirconium alloys and zirconium hydrides predicted from density functional perturbation theory," *Dalton Transactions*, 44, 18769-18779.